Direct numerical simulation of turbulent rotating Rayleigh–Bénard convection

R.P.J. Kunnen[1], B.J. Geurts[1,2] and H.J.H. Clercx[1,2]

[1] Fluid Dynamics Laboratory, Department of Physics, Eindhoven University of Technology, P.O. Box 513, 5600 MB Eindhoven, The Netherlands
R.P.J.Kunnen@tue.nl

[2] Department of Applied Mathematics, Faculty EEMCS, University of Twente, P.O. Box 217, 7500 AE Enschede, The Netherlands

Summary. The influence of rotation on turbulent convection is investigated with direct numerical simulation. The classical Rayleigh-Bénard configuration is augmented with steady rotation about the vertical axis. Correspondingly, characterization of the dynamics requires both the dimensionless Rayleigh number Ra and the Taylor number Ta. With increasing Ta the root-mean-square (rms) velocity-variations are found to decrease, while the rms temperature variations increase. Due to rotation a mean vertical temperature gradient develops, to partially compensate for the reduced convective heat transfer. Compared to the non-rotating case, at constant $Ra = 2.5\ 10^6$ the Nusselt number increases up to $\approx 5\%$ at relatively low rotation rates, $Ta < Ta_m \approx 10^6$, and decreases strongly when Ta is further increased. A striking change in the boundary layer structure arises when Ta traverses an interval about Ta_m, as is expressed by the near-wall vertical-velocity skewness.

1 Introduction

Rayleigh–Bénard convection is a classical problem in which a fluid layer enclosed between two parallel horizontal walls is heated from below. For small temperature differences between the plates there is no flow and heat is transported by conduction only. Above a certain temperature difference, convection sets in against the downward pointing gravitational acceleration, and a regular convection pattern is formed. At even higher temperature differences this pattern breaks down, eventually leading to plume-dominated turbulence [2].

In a rotating reference frame the Rayleigh-Bénard dynamics can be considerably modified through a combination of buoyancy and Coriolis forces. The Taylor–Proudman theorem implies that at sufficiently strong rotation rates flows are essentially two-dimensional. Hence, in general, rotation induces a dynamic competition between two- and three-dimensional tendencies in a convective flow. Rotating convection occurs in many geophysical and astrophysical settings, such as in Earth's atmosphere and in solar convection.

The dynamics of rotating Rayleigh–Bénard convection can be characterized by three dimensionless parameters, i.e., the Rayleigh number Ra, the Taylor number Ta, and the Prandtl number σ:

$$Ra = \frac{g\alpha\,\Delta T H^3}{\nu\kappa}\,, \quad Ta = \left(\frac{2\Omega H^2}{\nu}\right)^2\,, \quad \sigma = \frac{\nu}{\kappa}\,, \tag{1}$$

where g is the gravitational acceleration, α the thermal expansion coefficient, ν the kinematic viscosity, κ the thermal diffusivity, ΔT the temperature difference between the plates, H the separation between the horizontal walls, and Ω the rotation velocity.

While there is a considerable body of velocity and temperature measurements on non-rotating Rayleigh–Bénard convection [1], only a few measurements are reported for the rotating case [2, 3]. The effect of rotation on the total heat flux is usually expressed in terms of the Nusselt number Nu which depends in a complicated manner on (Ra, Ta, σ). In [4, 5], Ta and Ra were varied at constant Rossby number $Ro = \sqrt{Ra/(\sigma\,Ta)}$. A constant value of Ro essentially implies a fixed ratio between rotational and buoyancy effects. Only a modest increase of Nu was found at fixed Ro, in comparison to its value in the non-rotating system. Complementary, in [6, 7] Ta was varied independently of Ra. A slight increase of Nu at moderate Ta was observed while Nu decreases considerably at larger Ta.

The present study involves a separate variation of rotation rate, i.e. different Ta, at constant Ra and σ. Temperature and velocity statistics from direct numerical simulations (DNS) of turbulent rotating convection at $Ra = 2.5 \times 10^6$ and Prandtl number $\sigma = 1$ are considered. The Taylor number Ta varies between 0 and 2.3×10^7. These values of Ra and σ allow for direct comparison to the work of Julien et al. [4] who reported velocity and temperature statistics from a series of numerical simulations at $Ro = 0.75$. The range of Ta numbers provides for considerable rotational effects in the flow, while still meeting horizontal resolution requirements (see Sakai [8]).

This paper is organized as follows. In Sec. 2 the numerical method and its accuracy is discussed. The influence of rotation on velocity and temperature statistics is analyzed in Sec. 3. Concluding remarks can be found in Sec. 4.

2 Numerical method

The model incorporates the Boussinesq approximation in the Navier–Stokes and temperature equations for an incompressible rotating fluid [9]:

$$\frac{\partial \mathbf{u}}{\partial t} + (\mathbf{u}\cdot\nabla)\mathbf{u} + \left(\frac{\sigma Ta}{Ra}\right)^{1/2} \hat{\mathbf{z}} \times \mathbf{u} = -\nabla p + T\hat{\mathbf{z}} + \left(\frac{\sigma}{Ra}\right)^{1/2} \nabla^2 \mathbf{u}\,, \tag{2}$$

$$\frac{\partial T}{\partial t} + (\mathbf{u}\cdot\nabla)T = (\sigma Ra)^{-1/2} \nabla^2 T\,, \tag{3}$$

$$\nabla \cdot \mathbf{u} = 0\,, \tag{4}$$

where $\mathbf{u}$ is the velocity vector, $\hat{\mathbf{z}}$ the unit vector in vertical direction parallel to the axis of rotation, p the reduced pressure, and T the temperature. The equations have been made dimensionless with length scale H, a convective time scale $\tau = H/U$ based on the free-fall velocity $U = \sqrt{g\alpha\,\Delta T H}$, and temperature scale ΔT.

Equations (2)–(4) are solved on a rectilinear domain using the same boundary conditions as in [4]. In particular, the horizontal directions are periodic to approximately represent an infinite horizontal extent. At the top and bottom boundaries no-slip conditions are applied for velocity. The temperature is set to $T = 1$ at the lower wall, while at the upper wall $T = 0$. The discretization scheme is the symmetry-preserving finite-volume discretization as proposed in [10]. Preservation of symmetry in the difference operators ensures stability on any grid, and conservation of mass, momentum and kinetic energy when inviscid flow is concerned. Time-integration is done via a so-called one-leg (one evaluation of fluxes per time step) scheme similar to the popular Adams–Bashforth scheme. Values of Ta can be found in Table 1.

Table 1. All simulations adopt $Ra = 2.5 \times 10^6$ and $\sigma = 1$ while the Taylor numbers Ta are chosen such that buoyancy forces are either larger than Coriolis forces ($Ro > 1$) or smaller ($Ro < 1$).

Ta	0	1.6×10^5	2.4×10^5	4.0×10^5	1.4×10^6
Ro	∞	4.00	3.20	2.50	1.33
Ta		4.5×10^6	1.0×10^7	1.6×10^7	2.3×10^7
Ro		0.75	0.50	0.40	0.33

The sides of the computational domain are chosen to be $2 \times 2 \times 1$ in the two horizontal and in the normal directions respectively. The grid consists of 128^2 equidistant points horizontally, and vertically 64 unevenly spaced points are used. There is a higher density of grid points near the top and bottom walls in order to adequately resolve the thin viscous and thermal boundary layers. In all simulations the domain allows for at least four characteristic length scales in both horizontal directions [8]. A coarsening of the grid, as well as a change of the domain dimensions to $1 \times 1 \times 1$, induced no essential differences in the results which further underpins the selected resolution as well as the length of the periodic directions.

A simulation is initialized with zero velocity and a linear vertical temperature profile upon which small random perturbations are superimposed. After an initialization period of 50 dimensionless units, a statistically stationary state was found to have established itself after which the averaging-process was started. The averaging, denoted by $\langle\,.\,\rangle$, was carried out over horizontal grid-planes and time. Two quantities are of special interest for this study, i.e., the Nusselt number Nu and the vertical-velocity skewness S_w. The Nusselt number Nu involves the derivative of the average temperature at the wall [11]:

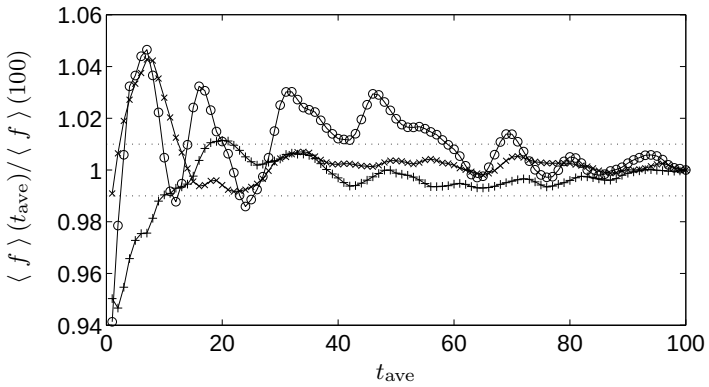

Fig. 1. Convergence of time-averaging at $Ta = RUDIE$. Scaled by their final values are given the maximum rms value of vertical velocity (*circles*), Nu calculated at the top wall (*crosses*), and Nu for the bottom wall (*pluses*). The 1% accuracy interval is indicated by the *dotted lines*.

$$Nu = \left. \frac{\partial \langle T \rangle}{\partial z} \right|_{\rm wall} . \tag{5}$$

This definition implies that the thermal boundary layers near the walls are adequately resolved, which necessitates the near-wall grid refinement. The skewness of vertical velocity S_w is defined as

$$S_w = \frac{\left\langle (w - \langle w \rangle)^3 \right\rangle}{\left\langle (w - \langle w \rangle)^2 \right\rangle^{3/2}} . \tag{6}$$

After averaging over 100 time-units the statistical convergence of the averaging process was observed to be within 1% relative error for Nu. This is illustrated in Fig. 1 for a characteristic simulation-setting. In particular, the running-time average of the maximum root-mean-square (rms) value of vertical velocity, scaled by its final value, and the convergence of Nu calculated at the bottom and top wall are shown.

3 Velocity and temperature statistics

The rms values of vertical and horizontal velocities as a function of the vertical coordinate are presented in Fig. 2. The rms horizontal velocity $u_{\rm rms}$ is defined following Kerr [11]

$$u_{\rm rms} = \sqrt{\langle (u - \langle u \rangle)^2 \rangle + \langle (v - \langle v \rangle)^2 \rangle} , \tag{7}$$

where $\langle u \rangle \approx \langle v \rangle \approx 0$ are included for generality. For $Ta = 0$ qualitative agreement is observed with profiles found by numerical simulations [11, 12] and

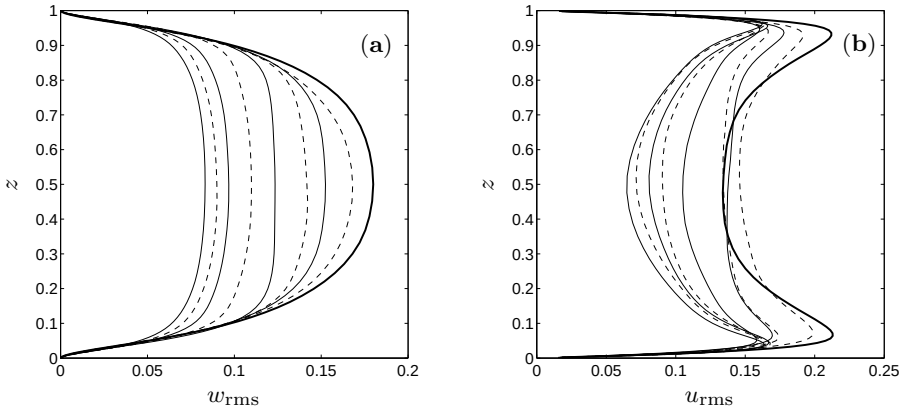

Fig. 2. (**a**) Vertical velocity rms as a function of the vertical coordinate. The non-rotating case ($Ta = 0$) is emphasized (*thick solid line*). From right to left Ta increases (*alternating dashed and solid lines*), see Table 1 for values. (**b**) Horizontal velocity rms as a function of the vertical coordinate. The line styles are the same as in (a), with Ta again increasing from right to left.

experiments [13], albeit at other Rayleigh and Prandtl numbers. In addition, we may directly compare the $Ro = 0.75$, $Ta = 4.5 \times 10^6$ case to the simulations of Julien et al. [4]. The rms vertical velocity at the mid-plane reported there is 0.108 (value adapted to the scaling used in this paper), while we obtain 0.110. Similarly, the temperature rms at the mid-plane is 0.0795 as reported by [4] (scaling adapted) compared to 0.0793 found here. These values show an excellent quantitative agreement within the time-averaging accuracy.

From Fig. 2 it is clear that at larger rotation rates the rms velocities near the centre are smaller, both horizontally and vertically. As Ta increases, the Rossby number Ro in the bulk decreases, thus indicating that the flow in the bulk is becoming more and more 'geostrophic', i.e., in this regime inertial and viscous forces are negligible when compared to the Coriolis force. The Taylor–Proudman theorem states that under such geostrophic conditions vertical motion is practically inhibited. The explanation for the decrease of horizontal velocity with increasing Ta has the same origin. At strong rotation the vertical motion is concentrated in coherent vertical vortex-tube structures. A radial flow towards the vortex tubes across the viscous boundary layers feeds the vortices. As the vertical motion is less intense, conservation of mass implies that the horizontal flow towards the vortices must also be smaller, hence the decrease of u_{rms} with increasing Ta.

The skewness of vertical velocity S_w, as defined in (6), is shown in Fig. 3. The non-rotating profile is very similar to the profiles found in numerical simulations by Kerr [11] and Moeng & Rotunno [12]. As is argued in [12] this skewness is a measure for the spatial distribution and importance of upward and downward motions in horizontal cross-sections. If there is a strong upward

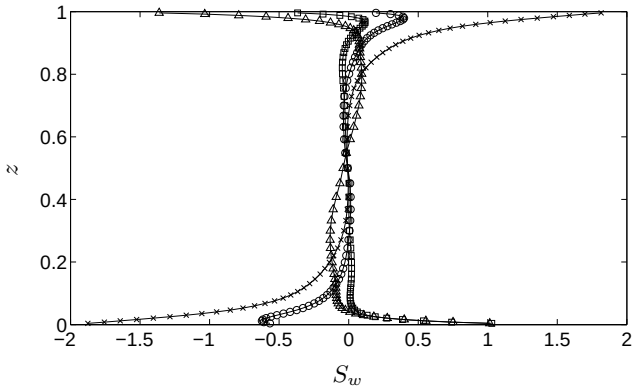

Fig. 3. Skewness of vertical velocity. For clarity only four curves are included: $Ta = 0$ (*crosses*), $Ta = 1.6 \times 10^5$ (*circles*), $Ta = 4.0 \times 10^5$ (*squares*), and $Ta = 1.4 \times 10^6$ (*triangles*). The higher-Ta curves are comparable to that at $Ta = 1.4 \times 10^6$.

motion that occupies only a small fraction of the cross-sectional area, a rather large positive skewness results. Similarly, a negative skewness is indicative of a strongly localized downward motion.

With increasing rotation rate, the near-wall skewness is seen to change sign, cf. Fig. 3. This indicates that the flow structures in rapidly rotating boundary layers differ essentially from the non-rotating case. In particular, the sign-change corresponds to a transition in which dominance of strongly localized downward motion 'switches' to a dominance of localized upward motion near the lower wall, and vice versa near the upper wall. This connects qualitatively to the strong thermal plumes that are observed in snapshots of the temperature field at high Ta. The structures in the boundary layers are highly influential to the thermal properties of the entire domain. Therefore, the effects of rotation on the flow-structures, especially in the boundary layers, is currently further investigated to quantify the above high-Ta switching.

In Fig. 4 the average temperature and its rms value as a function of the vertical coordinate are depicted. With increasing rotation there is a more pronounced temperature gradient over the bulk. In the non-rotating case there is hardly any temperature difference over the central region [11]. Julien et al. [4] provide an ingenious explanation for the persistence of the gradient. First they show that thermal plumes tend to have cyclonic vorticity, since the horizontal flow at the boundary layer toward a plume spins up cyclonically as a result of the Coriolis force. Then they note that in geostrophic turbulence like-signed vorticity regions tend to clump together [14]. The like-signed thermal vortices have a tendency to merge, thereby increasing lateral mixing. This lateral mixing causes the plumes to lose part of their heat while crossing the domain; a mean temperature gradient results. As the rotation increases, so does the vorticity associated with the thermal vortices. Hence, the tendency

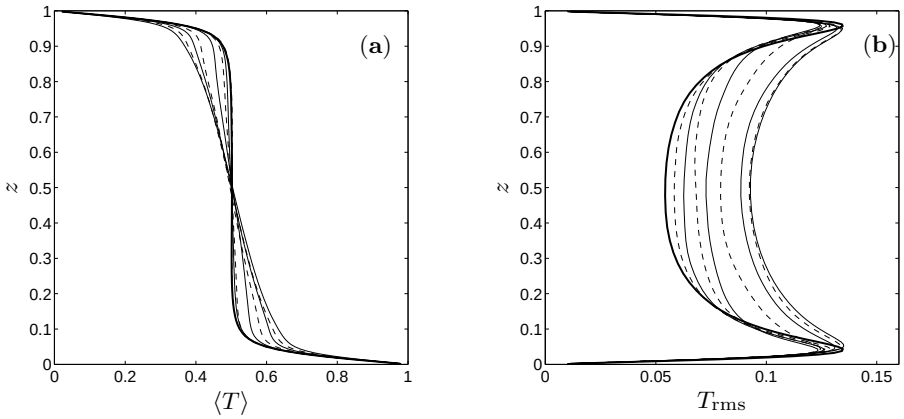

Fig. 4. (**a**) Average temperature. Line styles as in Fig. 2. *Ta* increases with increasing temperature gradient near the centre. (**b**) Temperature rms values as a function of the vertical coordinate. Line styles as in Fig. 2, with *Ta* now increasing from left to right.

to merge increases as well, as does lateral mixing and the vertical temperature gradient.

The mid-plane rms value of temperature increases with rotation, see Fig. 4(b). Apparently, the plumes moving vertically across the domain need a larger thermal contrast to counteract the suppression of vertical motion by rotation. Fernando et al. [3] experimentally found this result.

The dependence of the heat flux, as characterized by the Nusselt number, on the rotation rate is presented in Fig. 5. A remarkable feature is that *Nu*

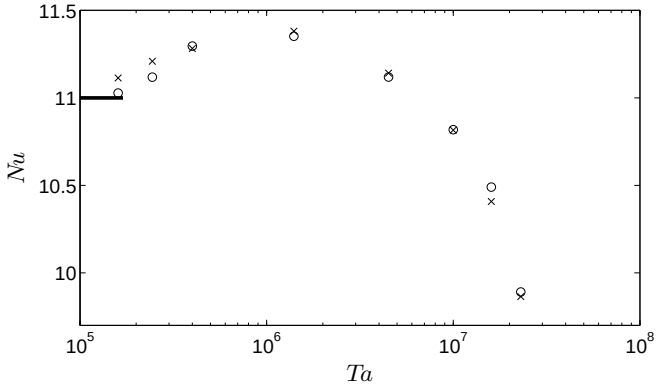

Fig. 5. Dependence of *Nu* on *Ta* in which *Nu* is calculated at the top wall (*crosses*) and at the bottom wall (*circles*). *Nu* for $Ta = 0$ is indicated on the vertical axis (*thick solid line*).

is increasing for $Ta \lesssim 10^6$, while decreasing at higher values. The simulations indicate that Nu appears to decay exponentially with increasing Ta. Similar behavior was also noticed in experiments in water ($\sigma = 6.8$) [6], with a maximum heat flux for $Ta = 3.0 \times 10^6$ at $Ra = 2.5 \times 10^6$.

Several authors [4, 5, 6, 15] note that Ekman pumping could account for the increased heat flux at moderate rotation rates. At larger rotation rates ($Ta \gtrsim 10^6$), however, the vertical motions are less intense and the convective heat flux is therefore reduced. It is expected that for $Ta \to \infty$ all convective motion will have ceased and that a purely conductive state ($Nu = 1$) remains with a constant temperature gradient over the fluid layer.

4 Concluding remarks

The influence of rotation on convective turbulence expresses itself in temperature and velocity statistics. An increase in rotation implies a decrease of rms velocities, while rms temperature fluctuations are increased. A vertical temperature gradient is maintained under rotation as opposed to the non-rotating case. At larger rotation rates the total heat flux through the fluid layer decreases. These changes can be explained through the suppression of vertical motion in the geostrophic bulk region. The vertical-velocity skewness shows a rather unexpected change under rotation, indicating a changing near-wall flow structure. A thorough investigation of the structures of motion with emphasis on the near-wall regions is currently carried out.

Acknowledgement. RPJK wishes to thank the Foundation for Fundamental Research of Matter (FOM) for financial support.

References

1. RUDIE: hier een algemeen RB overzicht (boek/artikel)
2. Vorobieff P, Ecke RE (2002) J Fluid Mech 458:191–218
3. Fernando HJS, Chen R-R, Boyer DL (1991) J Fluid Mech 228:513–547
4. Julien K, Legg S, McWilliams J, Werne J (1996) J Fluid Mech 322:243–273
5. Liu Y, Ecke RE (1997) Phys Rev Lett 79(12):2257–2260
6. Rossby HT (1969) J Fluid Mech 36(2):309–335
7. Pfotenhauer JM, Lucas PGJ, Donnelly RJ (1984) J Fluid Mech 145:239–252
8. Sakai S (1997) J Fluid Mech 333:85–95
9. Chandrasekhar S (1961) Hydrodynamic and Hydro-magnetic Stability. Oxford University Press
10. Verstappen RWCP, Veldman AEP (2003) J Comput Phys 187:343–368
11. Kerr RM (1996) J Fluid Mech 310:139–179
12. Moeng C-H, Rotunno R (1990) J Atmos Sci 47(9):1149–1162
13. Deardorff JW, Willis GE (1967) J Fluid Mech 28(4):675–704
14. McWilliams JC (1984) J Fluid Mech 146:21–43
15. Zhong F, Ecke RE, Steinberg V (1993) J Fluid Mech 249:135–159